

# A phenomenological study on single transverse-spin asymmetry for inclusive light-hadron productions at RHIC

Koichi Kanazawa<sup>1</sup> and Yuji Koike<sup>2</sup>

<sup>1</sup> *Graduate School of Science and Technology, Niigata University,  
Ikarashi, Niigata 950-2181, Japan*

<sup>2</sup> *Department of Physics, Niigata University, Ikarashi, Niigata 950-2181, Japan*

## Abstract

We study the single transverse-spin asymmetry for inclusive light-hadron productions in the proton-proton collision,  $p^\uparrow p \rightarrow hX$  ( $h = \pi, K, \eta$ ), for the RHIC kinematics based on the twist-3 mechanism in the collinear factorization. The analysis includes all the contributions from the soft-gluon-pole (SGP) and the soft-fermion-pole (SFP) for the twist-3 quark-gluon correlation functions in the transversely polarized proton. After discussing the flavor decomposition and the  $P_T$ -dependence of the asymmetry obtained in the previous analysis at the center-of-mass energy  $\sqrt{S} = 62.4$  and 200 GeV, we will give a prediction for the asymmetry at  $\sqrt{S} = 500$  GeV and also for the  $\eta$ -meson production. We found slightly smaller asymmetry at  $\sqrt{S} = 500$  GeV for  $\pi^{\pm,0}$  and  $K^+$  compared with those at the lower energies. The asymmetry for the  $\eta$ -meson turned out to be significantly larger than that for  $\pi^0$ .

# 1 introduction

In the last decades, large single transverse-spin asymmetries (SSA) in (semi-)inclusive reactions have been receiving much attention in high energy spin physics (for a recent review, see [1]). Since the large SSA can not occur in the conventional framework for the high-energy process based on the parton model and perturbative QCD, understanding the origin of SSA provides us with a new opportunity to reveal the nucleon structure and the QCD dynamics. One of the most conspicuous SSA is the one measured in the inclusive single-hadron production in the proton-proton collision:

$$p^\uparrow(p, S_\perp) + p(p') \rightarrow h(P_h) + X, \quad (1)$$

where  $S_\perp$  is the transverse spin vector of the polarized proton and  $h = \pi, K$  and  $\eta$  etc. The SSA for this process is characterized by  $A_N \equiv (\sigma^\uparrow - \sigma^\downarrow)/(\sigma^\uparrow + \sigma^\downarrow) \equiv \Delta\sigma/\sigma$ , where  $\sigma^\uparrow(\sigma^\downarrow)$  is the cross section obtained with the proton polarized along the spin vector  $S_\perp$  ( $-S_\perp$ ). The FNAL-E704 collaboration reported the first data for  $A_N$  for  $p^\uparrow p \rightarrow \pi X$  and  $\bar{p}^\uparrow p \rightarrow \pi X$  at the center-of-mass energy  $\sqrt{S} = 20$  GeV, which is as large as 30 % in the forward direction of the polarized proton or anti-proton [2, 3, 4]. RHIC at BNL also reported a similar magnitude of  $A_N$  at  $\sqrt{S} = 62.4, 200$  GeV [5, 6, 7, 8, 9, 10].

In our recent paper [11] (hereafter referred to as KK10), we have presented a numerical analysis of the RHIC  $A_N$  data for  $p^\uparrow p \rightarrow hX$  ( $h = \pi, K$ ) at  $\sqrt{S} = 62.4$  and 200 GeV in the framework of the collinear factorization. Since the unpolarized cross section for this process has been well-described by the next-to-leading order (NLO) QCD analysis in the collinear factorization [12], the analysis of  $A_N$  in the framework can be taken as a guide to clarify the origin of the asymmetry. In the collinear factorization, SSA appears as a twist-3 observable and is described in terms of multi-parton correlation functions [13, 14, 15]. (For the detailed formalism of the twist-3 calculation demonstrating the gauge invariance and the factorization property, see [15, 16, 17].) In KK10, we focused on the contribution from the quark-gluon correlation functions  $G_F^a(x_1, x_2)$  and  $\tilde{G}_F^a(x_1, x_2)$  with quark-flavor  $a$  ( $a = u, d, s, \bar{u}, \bar{d}, \bar{s}$ ) in the transversely polarized nucleon. They are defined from the light-cone correlation functions of the form  $\sim \langle \bar{\psi}^a g F^{\perp+} \psi^a \rangle$  in the nucleon, and  $x_1$  and  $x_2 - x_1$  represent, respectively, the light-cone momentum fractions carried by the quark and gluon lines coming out of the nucleon. These functions satisfy the symmetry property  $G_F^a(x_1, x_2) = G_F^a(x_2, x_1)$  and  $\tilde{G}_F^a(x_1, x_2) = -\tilde{G}_F^a(x_2, x_1)$ . (For the definition and the basic properties of these twist-3 functions, see KK10 and [15, 18].) In the twist-3 mechanism for SSA, the contribution from these two functions to the single-spin-dependent cross section  $\Delta\sigma$  occurs from a pole part of an internal propagator in the hard part, which reflects the naively  $T$ -odd nature of SSA. Such poles are classified into the soft-gluon-pole (SGP) and the soft-fermion-pole (SFP), which fix the momentum fractions at  $x_1 = x_2$  and  $x_i = 0$  ( $i = 1$  or 2), respectively. Due to the symmetry property,  $\tilde{G}_F^a$  does not contribute through SGP. Therefore the cross section can be written as [19, 20, 21, 22, 23]

$$\begin{aligned} \Delta\sigma = & \sum_{a,b,c} \left( G_F^a(x, x) - x \frac{dG_F^a(x, x)}{dx} \right) \otimes f^b(x') \otimes D^c(z) \otimes \hat{\sigma}_{ab \rightarrow c}^{\text{SGP}} \\ & + \sum_{a,b,c} \left( G_F^a(0, x) + \tilde{G}_F^a(0, x) \right) \otimes f^b(x') \otimes D^c(z) \otimes \hat{\sigma}_{ab \rightarrow c}^{\text{SFP}}, \end{aligned} \quad (2)$$

where  $f^b(x')$  is the twist-2 unpolarized parton distribution in the unpolarized nucleon and  $D^c(z)$  is the twist-2 unpolarized fragmentation function for the final hadron with the parton labels  $b$  and  $c$  ( $b, c = q, \bar{q}, g$ ). The scale dependence of each nonperturbative function is implicit. As shown in (2), the SGP contribution appears in the combination of  $G_F^a(x, x) - x \frac{dG_F^a(x, x)}{dx}$  [21, 22], while the SFP contribution appears in the form  $G_F^a(0, x) + \tilde{G}_F^a(0, x)$  [23]. In KK10, we have performed a fit of the RHIC  $A_N$  data for the pion and kaon productions based on Eq. (2) and found that the existing data have been well reproduced by the combination of the two effects. Although the main contribution is from the SGP contribution, the SFP contribution also plays an important role which can not be substituted by the SGP one.

The purpose of this paper is to report the details of the analysis in KK10 [11], in particular, the role of the SGP and SFP functions for each quark-flavor and the characteristic dependence of  $A_N$  on the final hadron's transverse momentum  $P_T$ , and to give a prediction for  $A_N$  at  $\sqrt{S} = 500$  GeV and also for the  $\eta$  meson, which are being measured at RHIC. Since we could not get a good fit by the SGP contribution only, we shall focus on the FIT 1 of KK10 which includes both SGP and SFP contributions in this paper. This analysis used the GRV98 for the unpolarized parton distribution [24] and the DSS fragmentation function [25] for  $\pi$  and  $K$ . During the present study, we found that the cross section formula for the SGP contribution used in KK10 (Eq.(6) of [11]) has an error in the overall sign.<sup>1</sup> Accordingly, the sign of the obtained SGP functions should be reversed, while the SFP functions stay the same. With this change all the results for the asymmetries in KK10 remain the same.

## 2 Flavor structure of the asymmetry

We begin our discussion by the flavor structure of the asymmetry for  $\pi^{\pm,0}$  and  $K^{\pm}$ . In Fig. 1, we show the decomposition of  $A_N$  into the SGP and SFP contributions for each quark and anti-quark flavor. The left panels show the decomposition of  $A_N$  into the total SGP and SFP contributions, while the right panels show the contribution from each quark and anti-quark flavor both for the SGP and SFP contributions. To understand the pattern of the flavor structure, we show the SGP and SFP functions obtained in FIT 1 of KK10 for each quark and anti-quark flavor in Fig. 2, by correcting the sign error mentioned at the end of the introduction. First, as seen in the top two panels of Fig. 1, the major contributions for  $\pi^{\pm}$  come from the SGP components for the favored quark flavors:  $A_N$  for  $\pi^+$  is dominated by the SGP contribution for the  $u$  and  $\bar{d}$  quarks, and  $A_N$  for  $\pi^-$  is dominated by that for the  $d$  and  $\bar{u}$  quarks. Note here the significance of the  $\bar{u}$  and  $\bar{d}$  components, which results from the large SGP functions for these “sea” flavors in the nucleon at large  $x$  as shown in Fig. 2. The net SFP effect turned out to be small for  $\pi^{\pm}$  in the region of  $x_F > 0.4$  for which the RHIC data are available. If one looks into more details of the SFP contribution, the SFP effect brings some net effect for  $\pi^-$ , while it is much smaller for  $\pi^+$ . This feature of the SFP contribution can also be seen for  $K^{\pm}$ . (See discussions below.) The above feature of the SGP dominance can also be seen in  $A_N$  for  $\pi^0$ : All the SGP contributions from  $u$ ,  $d$ ,  $\bar{u}$  and  $\bar{d}$  bring large contributions to  $A_N^{\pi^0}$  in the large  $x_F$  region. The net SFP effect can be found in the small  $x_F$  region for  $\pi^0$ : It brings some effect at  $x_F < 0.4$  which cancels the

---

<sup>1</sup>By this change, our SGP cross section formula becomes consistent with what is claimed in a recent paper [26].

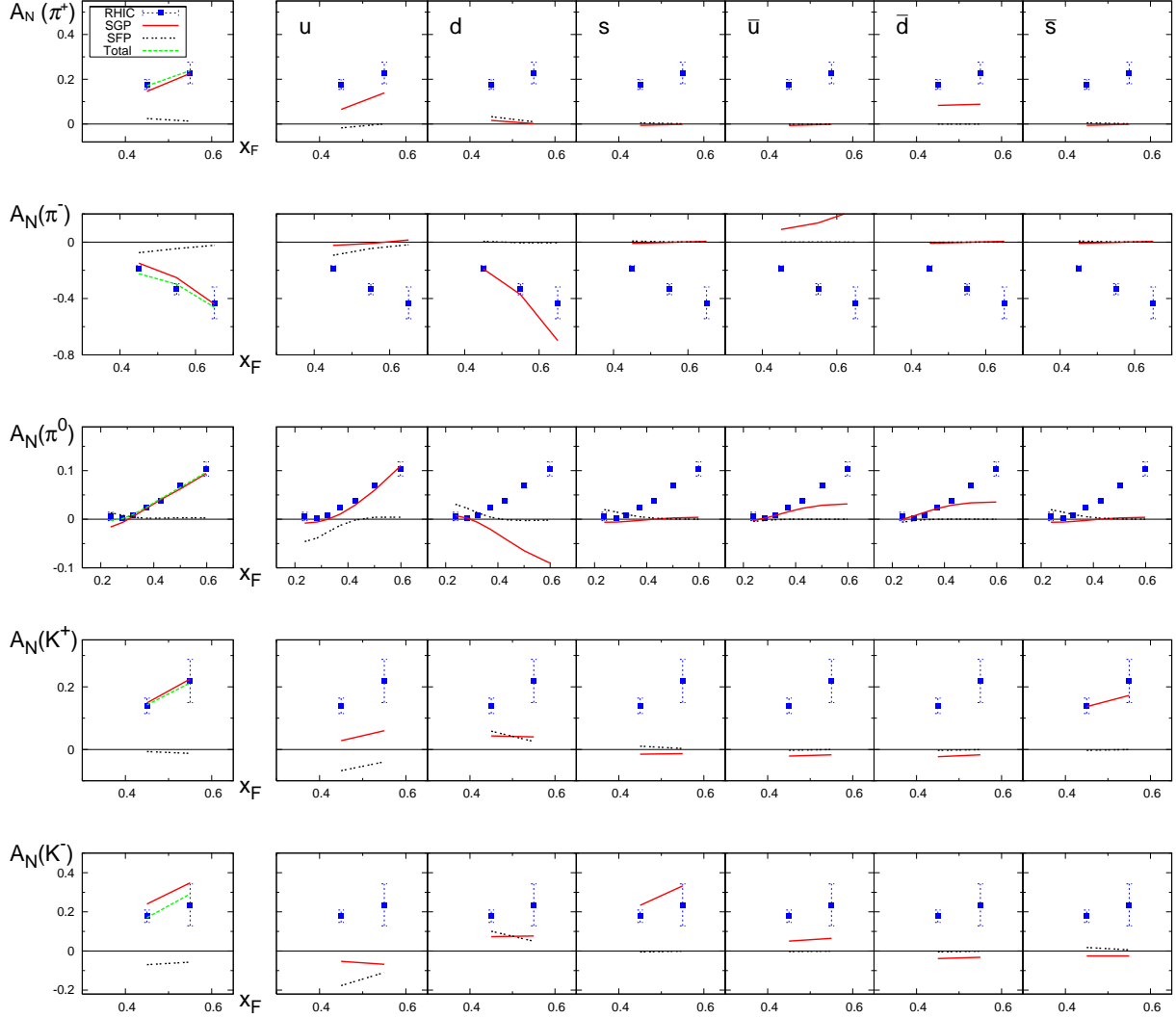


Figure 1: Decomposition of  $A_N$  at  $x_F > 0$  obtained in FIT 1 of KK10 [11] into the SGP and SFP contributions (left panels) which are decomposed further into each quark-flavor component (right panels). The solid and dotted lines show the contributions from the SGP and SFP components, respectively. The dashed line in the left panels show the total  $A_N$ . Data points from RHIC [7, 8] are also shown.

SGP contribution, making the  $A_N$  small. This feature can be understood if one remembers that the partonic hard cross section for SFP is much larger than that for SGP in many relevant channels, although the derivative of the SGP function enhances its contribution.

The twist-3 functions for the sea quark flavors in the nucleon become more important for the kaons. In particular, the observed large  $A_N$  for  $K^-$  should come from the sea quarks due to its flavor structure,  $K^- \sim \bar{u}s$ . As seen in Fig. 1, the largest contribution to  $A_N$  for  $K^+$  and  $K^-$  comes from the SGP functions for the  $\bar{s}$  and  $s$  quarks, respectively, and for  $K^+$  even the SGP contribution from the  $u$ -quark is significantly smaller than that from the  $\bar{s}$ -quark. This is due to the much larger strangeness component for the kaon in the DSS fragmentation function as well as the sizable magnitude of the SGP functions for the  $s$  and

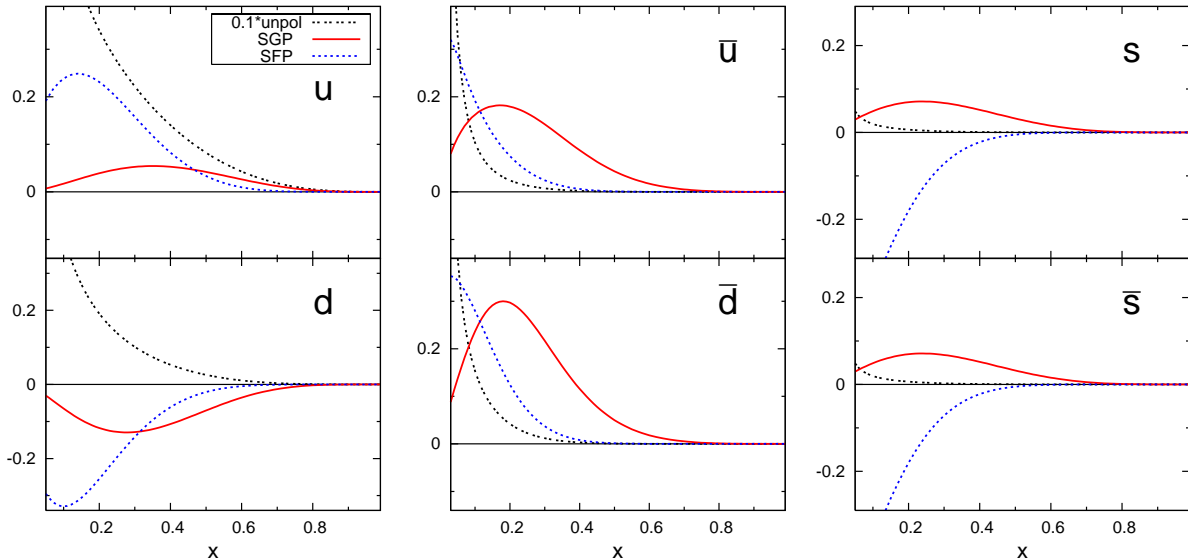


Figure 2: The SGP function  $G_F^a(x, x)$  and the SFP function  $G_F^a(0, x) + \tilde{G}_F^a(0, x)$  at the scale  $\mu^2 = 2.4 \text{ GeV}^2$  for each quark-flavor obtained in FIT 1 of KK10 in comparison to the unpolarized quark distribution  $f_a(x)$  [scaled by factor 1/10].

$\bar{s}$  quarks in the nucleon. Combined with the result for the pions, one may say that  $A_N$  for the pions and kaons reflects the flavor structure of the fragmentation functions rather than that of the SGP functions. This is in contrast to the unpolarized cross section where the contribution from the valence quark flavors in the nucleon dominate in the forward rapidity region.

The contribution of the SFP effect shows a very different pattern from the SGP contribution. As shown in Fig. 1, the net SFP effect survives for  $K^-$  and  $\pi^-$  at  $x_F > 0.4$ , while it is negligible for  $K^+$  and  $\pi^+$ . This net effect for the former is caused by the SFP function for the  $u$ -quark flavor through the gluon fragmentation channel in combination with the large gluon component in the DSS fragmentation function, in particular, for the kaon. (The SFP function for the  $d$ -quark is also large and partly cancels the  $u$ -quark contribution. However, the  $u$ -quark function has longer range than the  $d$ -quark function, and thus the former effect is larger.) As shown in [23], the SFP partonic hard cross section in the gluon fragmentation channel is extremely large and has opposite sign compared with that in the quark fragmentation channel. For  $K^+$  and  $\pi^+$ , the  $u$ -quark SFP contribution in the gluon-fragmentation channel is mostly canceled by that in the  $u$ -quark fragmentation channel for which  $K^+$  and  $\pi^+$  have a large fragmentation functions as a favored flavor, while the former contribution is not canceled by the latter for  $K^-$  and  $\pi^-$ . To see this feature, we showed in Fig. 3 the decomposition of the SGP and SFP contribution for the  $u$ -quark into the quark fragmentation channel and the gluon fragmentation channel. As seen from this figure, the  $u$ -quark SFP contribution via the gluon fragmentation channel survive for  $K^-$  and  $\pi^-$ , while they are canceled by that via the quark fragmentation channel for  $K^+$  and  $\pi^+$ .

Summarizing the flavor structure of  $A_N$ , the SGP contribution for the favored quark flavors is the dominant one, while the SFP contribution for the valence  $u$  and  $d$  quarks is also significant via the gluon fragmentation channel. This SFP effect survive for  $K^-$  and

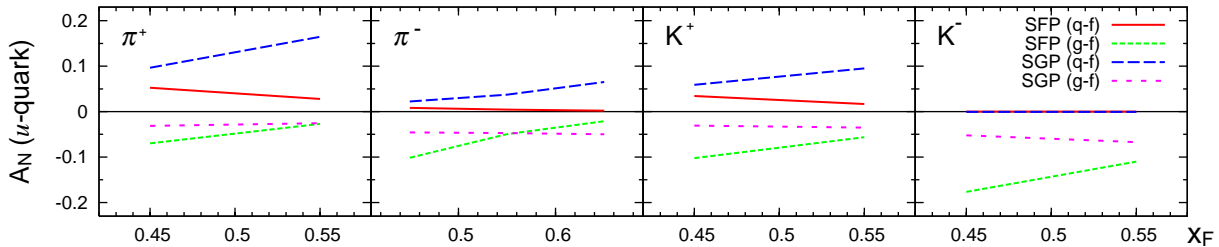


Figure 3: Decomposition of the  $u$ -quark SGP and SFP contribution to  $A_N$  at  $\sqrt{S} = 62.4$  GeV shown in Fig. 1 into the quark and gluon fragmentation channel.

$\pi^-$  but is canceled by that in the quark-fragmentation channel for  $K^+$  and  $\pi^+$ .

### 3 $P_T$ -dependence

The  $P_T$ -dependence of  $A_N$  provides an important test for the mechanism of the asymmetry. In Ref. [11], we have found that our predictions for the  $\pi^0$  production shows a good agreement with the RHIC-STAR data at  $\sqrt{S} = 200$  GeV. In Fig. 4, we show the  $P_T$ -dependence of  $A_N$  for  $\pi^0$  in the wider range of  $P_T$  at  $x_F = 0, 0.28, 0.37$  and  $0.50$  together with the RHIC-PHENIX data at  $x_F = 0$  [6]. As seen in the figure, calculated  $A_N$  at  $x_F = 0$  stays zero in the whole  $P_T$  region, which is in agreement with the PHENIX data.

A conspicuous feature of the  $P_T$ -dependence is that the calculated  $A_N$  once increases up to  $P_T \sim$  a few GeV and then decreases slowly, which is in agreement with the STAR data. This behavior is in conflict with our naive expectation that  $A_N$  should behaves like  $1/P_T$  as a function of  $P_T$  by reflecting its twist-3 nature. We have found that the contribution from the gluon fragmentation channels plays an important role to cause this peculiar  $P_T$ -dependence of  $A_N$ . It brings negative contribution to the positive polarized cross section  $\Delta\sigma$  which is the numerator of  $A_N$ , while it brings positive one to the unpolarized cross section  $\sigma$ . With the DSS fragmentation function used which has a large gluon component, their contributions decrease very rapidly as the scale  $\mu = P_T$  becomes higher. Correspondingly,  $\Delta\sigma$  decreases relatively slowly around  $P_T \simeq 1 - 3$  GeV compared with the denominator, even though the twist-3 cross section accompanies the factor  $1/P_T$ . Such behavior is absent in the previous study by Kouvaris *et al* [21] which used Kretzer's fragmentation function [27] whose gluon fragmentation function is small. For comparison we calculated  $A_N$  by fixing the scale of the distribution and fragmentation functions at  $\mu = 1$  GeV (instead of  $\mu = P_T$ ) and found that  $A_N$  decreases monotonously as  $P_T$  increases and diverge toward  $P_T \rightarrow 0$ .

Another interesting point in Fig. 4 is that  $A_N$  does not decrease as fast as  $1/P_T$  in the high  $P_T$  region. This is because of the coexistence of the two effects proportional to  $M_N P_T / (-T)$  and  $M_N P_T / (-U)$  in the twist-3 asymmetry where  $T = (p - P_h)^2$  and  $U = (p' - P_h)^2$  are the Mandelstam variables: While the former effect is much larger at small  $P_T$ , the latter also brings significant contribution at large  $P_T$ .

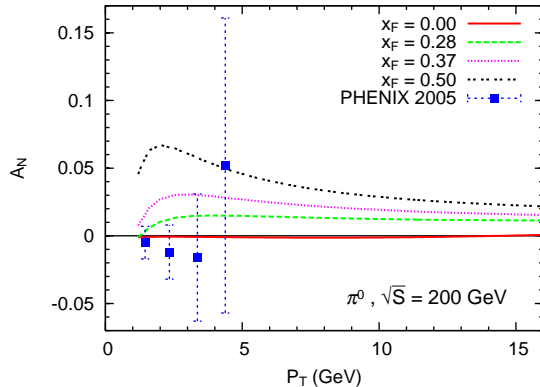


Figure 4:  $P_T$ -dependence of  $A_N^{\pi^0}$  at  $\sqrt{S} = 200$  GeV and four fixed  $x_F$  together with the PHENIX data at  $x_F = 0$  [6].

## 4 $A_N$ at $\sqrt{S} = 500$ GeV

Since the measurement of  $A_N$  is being extended to  $\sqrt{S} = 500$  GeV at RHIC, we present a prediction for  $A_N$  at this energy, using the SGP and SFP functions obtained from the data at  $\sqrt{S} = 200$  and 62.4 GeV.

In Fig. 5, we show the result of  $A_N$  for pions and kaons as a function of  $x_F$  for the pseudorapidity  $\eta = 3.6$  and  $\eta = 4.0$ . For the pions, the general trend of the asymmetry is the same as those at lower energies, while the magnitude of the asymmetry becomes smaller at each  $x_F$ . This is because a larger value of  $\sqrt{S}$  corresponds to larger  $P_T$  for a fixed  $x_F$  and thus the polarized cross section is more power suppressed at higher  $\sqrt{S}$ .

$A_N$  for kaons turned out to become larger than those for charged pions in the large  $x_F$  region, in particular, for the  $K^-$  meson. This larger  $A_N$  for  $K^\pm$  is mainly due to the faster decrease of the unpolarized cross section for the  $K^\pm$  production compared with the  $\pi^\pm$  production with increasing  $\sqrt{S}$  from 62.4 GeV to 500 GeV. This decrease of the unpolarized cross section becomes even more manifest for the  $K^-$  production, since the unpolarized cross section in the forward region is dominated by the contribution from the valence flavors in the nucleon and the sea contribution is more suppressed at higher scale  $\mu = P_T$  at large  $x_F$ . Therefore  $A_N$  for  $K^-$  becomes much larger than that for  $K^+$ . We found that  $A_N$  for  $K^-$  overshoots one in the large  $x_F$  region. In our present analysis, the constraint on the SGP and SFP functions for the  $s$  and  $\bar{s}$  quarks comes only from a very limited number of the kaon data with the assumption that they are the same for the  $s$  and  $\bar{s}$  quarks. With more number of data points, this unfavorable feature should be corrected. Nevertheless, we expect the relation  $A_N^{K^-} > A_N^{K^+} \geq A_N^{\pi^+}$  at  $\sqrt{S} = 500$  GeV by the reason stated above.

Finally we show in Fig. 6 the  $P_T$ -dependence of  $A_N$  for  $\pi^0$  at  $\sqrt{S} = 500$  GeV. As in the case of  $\sqrt{S} = 200$  GeV,  $A_N$  once increases toward  $P_T \simeq$  a few GeV and then decreases slowly.

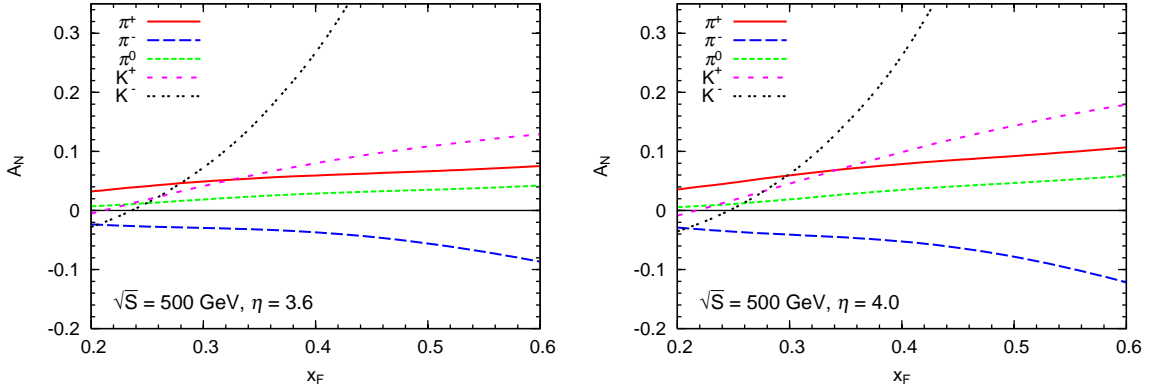


Figure 5:  $A_N$  for pions and kaons at  $\sqrt{S} = 500$  GeV and the pseudorapidity  $\eta = 3.6$  (left) and  $\eta = 4.0$  (right).

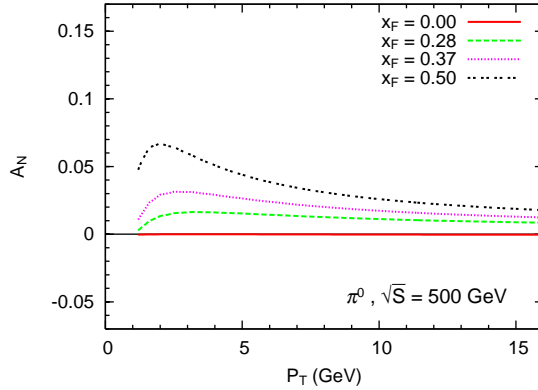


Figure 6:  $P_T$ -dependence of  $A_N^{\pi^0}$  for  $\sqrt{S} = 500$  GeV at  $x_F = 0, 0.28, 0.37$  and  $0.5$ .

## 5 $A_N$ for $\eta$ meson

The first data of  $A_N$  for the  $\eta$ -meson production was reported by the FNAL-E704 collaboration for the  $pp$  and  $\bar{p}p$  collisions [4]. They found a clear indication that  $A_N^\eta$  for the  $pp$  collision is positive and substantially larger than  $A_N^{\pi^0}$ . Recently the RHIC-STAR collaboration reported a preliminary data for  $A_N^\eta$  at  $\sqrt{S} = 200$  GeV, which also shows  $A_N^\eta$  is larger than  $A_N^{\pi^0}$  in the large  $x_F$  region by about factor two or more [9]. Here we present an estimate for  $A_N^\eta$  based on Eq. (2) using the SGP and SFP functions obtained in KK10. In this scenario, the difference between  $A_N^\eta$  and  $A_N^{\pi^0}$  comes from the difference between the difference in the fragmentation functions. As the fragmentation function for the  $\eta$ -meson, we adopt the recent AESSS parametrization [28] which is obtained by the next-to-leading order (NLO) QCD analysis of the existing data, assuming the equal contributions from all quark and anti-quark flavors as  $D_u^\eta = D_{\bar{u}}^\eta = D_d^\eta = D_{\bar{d}}^\eta = D_s^\eta = D_{\bar{s}}^\eta$ . Although we used the leading-order (LO) formula for the twist-3 cross section (2), we use the above only available



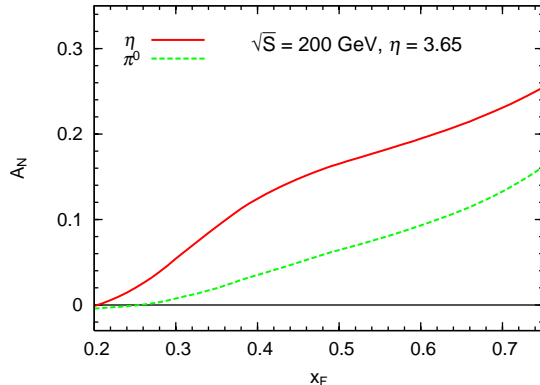


Figure 7:  $A_N$  for the  $\eta$ -meson at  $\sqrt{S} = 200$  GeV and the pseudorapidity  $\eta = 3.65$  in comparison with  $A_N$  for  $\pi^0$ .

NLO parametrization for the  $\eta$ -fragmentation function in this first study of  $A_N^\eta$ .<sup>2</sup>

Fig. 7 shows the calculated  $A_N^\eta$  as a function of  $x_F$  in comparison with  $A_N^{\pi^0}$  at  $\sqrt{S} = 200$  GeV and  $\eta = 3.65$ . In the large  $x_F$  region,  $A_N^\eta$  is approximately 1.5 times larger than  $A_N^{\pi^0}$ . This is consistent with the observed tendency of  $A_N^\eta$  at RHIC, although its magnitude still seems insufficient to explain the RHIC-STAR data [9]. As in the case of  $A_N^{\pi^0}$ , the SGP contribution dominates  $A_N^\eta$ . To see the origin of the difference between  $A_N^\eta$  and  $A_N^{\pi^0}$ , we have shown in Fig. 8 the decomposition of the SGP contribution to  $A_N^\eta$  and  $A_N^{\pi^0}$  into the contribution from each fragmentation channel. From this figure, one sees that the difference between the two mesons comes from the large contribution in the strangeness fragmentation channel for the  $\eta$ -meson. This large strangeness contribution is caused by the combination of the large strangeness component in the  $\eta$ -meson fragmentation function and the large SGP functions for  $s$  and  $\bar{s}$  which were responsible for  $A_N^{K^\pm}$ . Therefore in the present analysis, there is a strong correlation between the large  $A_N$  for the kaon and the  $\eta$ -meson. As another possible origin of the difference between  $A_N^\eta$  and  $A_N^{\pi^0}$ , the twist-3 fragmentation function may contribute [29], for which the complete cross section formula is not available yet. This effect may explain the remaining difference between the two asymmetries. For the complete clarification of the asymmetries, one needs to perform a global analysis of more variety of data using the complete cross section formula, which is beyond the scope of this study.

## 6 Summary

In this paper, we have studied the SSA for the inclusive pion, kaon and  $\eta$ -meson productions in the  $pp$  collision at typical kinematical regime of RHIC, using the SGP and SFP functions for the twist-3 quark-gluon correlation functions obtained in our previous analysis. We first discussed the role of the SGP and SFP functions for each quark and anti-quark flavor. It turned out that the SGP contributions from both “valence” and “sea” flavors in the

<sup>2</sup>Since the LO and NLO parametrizations for  $\pi$  in [25] are not very different from each other, we expect the use of LO fragmentation function for  $\eta$  would not cause much error.

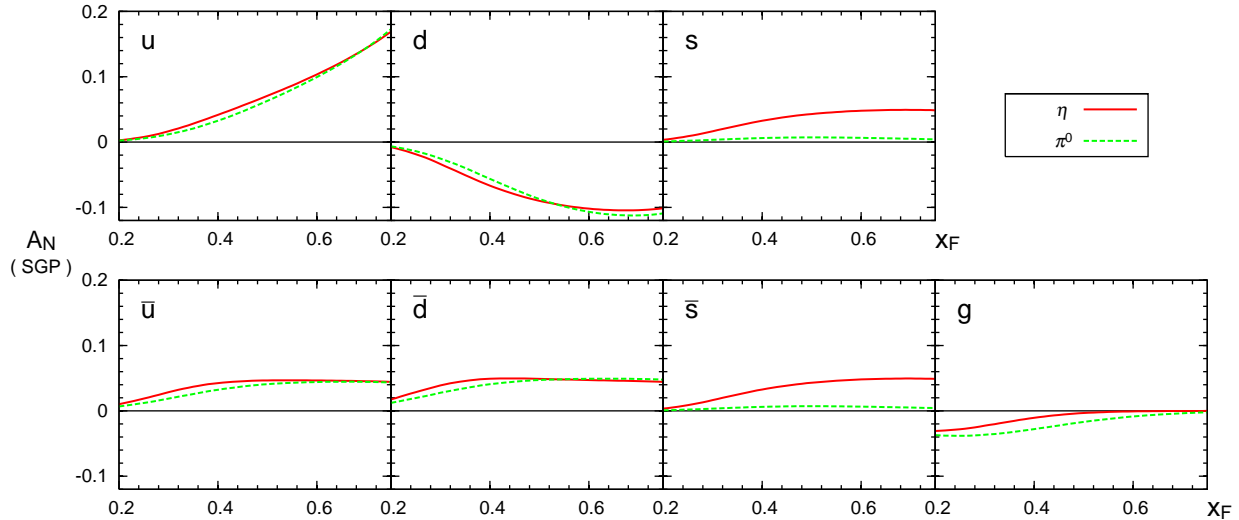


Figure 8: Decomposition of  $A_N^\eta$  and  $A_N^{\pi^0}$  into each fragmentation channel at  $\sqrt{S} = 200$  GeV and the pseudorapidity  $\eta = 3.65$ .

nucleon play an important role to reproduce the observed pattern of the asymmetries, and that the main contribution to  $A_N$  for each meson reflects more the flavor content in the DSS fragmentation function. Our analysis reproduces the observed  $P_T$ -dependence of RHIC  $A_N$  data for  $\pi^0$ . We found that the large contribution from the gluon fragmentation channel both in the unpolarized and polarized cross sections plays a crucial role to cause the peculiar behavior of  $A_N$  around  $P_T \simeq$  a few GeV.

We also presented a prediction of  $A_N$  for the kaons and pions at  $\sqrt{S} = 500$  GeV, which is being measured at RHIC. We found a slightly smaller asymmetries for the pion compared with those at  $\sqrt{S} = 62.4$  and 200 GeV. For the kaons,  $A_N$  was found to become larger than those for the pions in the large  $x_F$ -region at  $\sqrt{S} = 500$  GeV, especially  $A_N$  for  $K^-$  becomes much larger because of the small unpolarized cross section.  $A_N$  for the  $\eta$ -meson turned out to be larger than that for  $\pi^0$  by about factor 1.5, which partially explains the tendency of the RHIC data. This larger  $A_N$  originates from the large strangeness fragmentation function for the  $\eta$  meson combined with the sizable strangeness SGP function in the polarized nucleon.

Present analysis is based on the assumption that the whole  $A_N$  for  $p^\uparrow p \rightarrow hX$  ( $h = \pi, K$  and  $\eta$ ) originates from the twist-3 quark-gluon correlation functions in the polarized nucleon. To determine these functions, the SSA data on the Drell-Yan process and the direct-photon production in the  $pp$ -collision is extremely useful, since there is no fragmentation ambiguity associated with the final hadron in these processes. For the complete understanding of SSAs, a global analysis of variety of processes based on the complete formula is needed.

## Acknowledgements

We thank C. A. Aidala and M. Stratmann for their correspondence and providing their fortran code of the fragmentation function for  $\eta$ -meson.

## References

- [1] V. Barone, F. Bradamante, and A. Martin, *Prog. Part. Nucl. Phys.* **65**, 267 (2010).
- [2] Fermilab E704 Collaboration, D. L. Adams *et al.*, *Phys. Lett. B* **261**, 201 (1991).
- [3] Fermilab E704 Collaboration, D. L. Adams *et al.*, *Phys. Lett. B* **264**, 462 (1991).
- [4] Fermilab E704 Collaboration, D. L. Adams *et al.*, *Nucl. Phys. B* **510**, 3 (1998).
- [5] STAR Collaboration, J. Adams *et al.*, *Phys. Rev. Lett.* **92**, 171801 (2004).
- [6] PHENIX Collaboration, S. S. Adler *et al.*, *Phys. Rev. Lett.* **95**, 202001 (2005).
- [7] STAR Collaboration, B. I. Abelev *et al.*, *Phys. Rev. Lett.* **101**, 222001 (2008).
- [8] BRAHMS Collaboration, I. Arsene *et al.*, *Phys. Rev. Lett.* **101**, 042001 (2008).
- [9] STAR Collaboration, S. Heppelmann, arXiv:0905.2840 [nucl-ex].
- [10] PHENIX Collaboration, A. Adare *et al.*, *Phys. Rev. D* **82**, 112008 (2010).
- [11] K. Kanazawa and Y. Koike, *Phys. Rev. D* **82**, 034009 (2010).
- [12] B. Jäger, A. Schäfer, M. Stratmann, and W. Vogelsang, *Phys. Rev. D* **67**, 054005 (2003).
- [13] A. V. Efremov and O. V. Teryaev, *Sov. J. Nucl. Phys.* **36**, 140 (1982).
- [14] J. Qiu and G. Sterman, *Nucl. Phys. B* **378**, 52 (1992).
- [15] H. Eguchi, Y. Koike, and K. Tanaka, *Nucl. Phys. B* **763**, 198 (2007).
- [16] Y. Koike and K. Tanaka, *Phys. Lett. B* **646**, 232 (2007); **668**, 458(E) (2008).
- [17] H. Beppu, Y. Koike, K. Tanaka, and S. Yoshida, *Phys. Rev. D* **82**, 054005 (2010).
- [18] H. Eguchi, Y. Koike, and K. Tanaka, *Nucl. Phys. B* **752**, 1 (2006).
- [19] J. Qiu and G. Sterman, *Phys. Rev. D* **59**, 014004 (1998).
- [20] Y. Kanazawa and Y. Koike, *Phys. Lett. B* **490**, 99 (2000).
- [21] C. Kouvaris, J.-W. Qiu, W. Vogelsang, and F. Yuan, *Phys. Rev. D* **74**, 114013 (2006).
- [22] Y. Koike and K. Tanaka, *Phys. Rev. D* **76**, 011502 (2007).
- [23] Y. Koike and T. Tomita, *Phys. Lett. B* **675**, 181 (2009).
- [24] M. Glück, E. Reya, and A. Vogt, *Eur. Phys. J. C* **5**, 461 (1998).
- [25] D. de Florian, R. Sassot, and M. Stratmann, *Phys. Rev. D* **75**, 114010 (2007).
- [26] Z.-B. Kang, J.-W. Qiu, W. Vogelsang, and F. Yuan, arXiv:1103.1591 [hep-ph].
- [27] S. Kretzer, *Phys. Rev. D* **62**, 054001 (2000).

- [28] C. A. Aidala, F. Ellinghaus, R. Sassot, J. P. Seele, and M. Stratmann, Phys. Rev. D **83**, 034002 (2011).
- [29] Z.-B. Kang, F. Yuan, and J. Zhou, Phys. Lett. B **691**, 243 (2010).